



## **Gravitactic Swimming of the Planula Larva of the Coral Acropora: Characterization of Straightforward Vertical Swimming**

Authors: Takeda-Sakazume, Asuka, Honjo, Junko, Sasano, Sachia, Matsushima, Kanae, Baba, Shoji A., et al.

Source: Zoological Science, 40(1) : 44-52

Published By: Zoological Society of Japan

URL: <https://doi.org/10.2108/zs220043>

---

BioOne Complete ([complete.BioOne.org](https://complete.BioOne.org)) is a full-text database of 200 subscribed and open-access titles in the biological, ecological, and environmental sciences published by nonprofit societies, associations, museums, institutions, and presses.

Your use of this PDF, the BioOne Complete website, and all posted and associated content indicates your acceptance of BioOne's Terms of Use, available at [www.bioone.org/terms-of-use](https://www.bioone.org/terms-of-use).

Usage of BioOne Complete content is strictly limited to personal, educational, and non - commercial use. Commercial inquiries or rights and permissions requests should be directed to the individual publisher as copyright holder.

---

BioOne sees sustainable scholarly publishing as an inherently collaborative enterprise connecting authors, nonprofit publishers, academic institutions, research libraries, and research funders in the common goal of maximizing access to critical research.

# Gravitactic Swimming of the Planula Larva of the Coral *Acropora*: Characterization of Straightforward Vertical Swimming

Asuka Takeda-Sakazume, Junko Honjo, Sachia Sasano<sup>†</sup>, Kanae Matsushima, Shoji A. Baba, Yoshihiro Mogami, and Masayuki Hatta<sup>\*</sup>

*Department of Biology, Graduate School of Humanities and Sciences, Ochanomizu University, Tokyo 112-8610, Japan*

Vertical migration as well as horizontal dispersion is important in the ecological strategy of planktonic larvae of sedentary corals. We report in this paper unique vertical swimming behavior of planulae of the reef-building coral *Acropora tenuis*. Several days after fertilization, most of the planulae stayed exclusively at either the top or the bottom of the rearing tank. A good proportion of the planulae migrated almost vertically between top and bottom with fairly straight trajectories. Planulae sometimes switched their swimming direction via a sharp turn between the opposite directions. Quantitative analyses demonstrated that planulae kept constant speed while swimming either upward or downward, in contrast to frequent changes of direction and speed in horizontal swimming. Statistical comparison of propulsive speeds, estimated from swimming speeds and passive sedimentation, revealed gravikinesis of planulae, where the propulsive speed was significantly greater in downward swimming than upward swimming. The larval density hydrodynamically estimated was 0.25% lower than sea water density, which might be explained by the large quantity of lipids in planulae. Also, the deciliated larvae tended to orient oral end-up during floatation, presumably due to asymmetrical distribution of the endogenous light lipids. Plasticity of the larval tissue geometry could easily cause relocation of the center of forces which work together to generate gravitactic-orientation torque and, therefore, abrupt changing of the gravitactic swimming direction. The bimodal gravitactic behavior may give a new insight into dispersal and recruitment of coral larvae.

**Key words:** *Acropora*, coral, gravikinesis, gravitaxis, planula

## INTRODUCTION

Dispersal of propagules is critical for sedentary marine invertebrates to expand their habitats. Among such dispersals of propagules, the dispersal of planktonic larvae of reef-building corals has recently held worldwide attention following the rapid decline of coral reefs all over the globe. Larval dispersal and settlement must be important keys for maintenance and recovery of coral reefs, as shown in many research reports on recruitment and extensive genetic connectivity (e.g., Nakajima et al., 2012). The genus *Acropora* has been especially focused on according to its importance in reef ecosystems as a dominant pioneer species due to its rapid growth and high reproducibility. However, processes of dispersal and recruitment of acroporids' larvae have been understood in a simple scheme: eggs of acroporid corals are buoyant, and the resultant planula larvae gradually go down to the seabed to settle down on appropriate substrata after dispersion mostly by horizontal advection in the ocean

(Storlazzi et al., 2017). The vertical component of motion has been assessed mainly as free-fall, which physically biases the swimming behavior in the course of ontogeny (Martinez-Quintana et al., 2015; Guizien et al., 2020), simply driven by an irreversible loss of buoyancy due to consumption of the light fatty content (Arai et al., 1993). If the vertical migration process is a one-way trip, planulae have to find settlement positions at the first landing place. Those larvae which fail to fall onto an appropriate substratum have no chance to proceed to their sedentary life. In contrast, if planulae are capable of repeating vertical migration, they could return from inappropriate substrata to the water surface, where they would drift again, and probably have a chance of attempting a subsequent settlement. The latter scenario is beneficial for planulae which have a remarkable ability to drift for more than a month (Harii et al., 2007) and a strict preference regarding their settlement environment (Morse et al., 1996).

We observed frequent straight swimming of acroporid's planulae by ciliary beating both in downward and upward directions when rearing them in a transparent bucket 20 cm deep. The vertical swimming was continued from the water surface to the bottom, and vice versa. Although no distinct tissues or organs for gravity reception appeared to differentiate in planulae, which consist of a simple layer of ectodermal cells with diffuse neurons and unorganized endodermal

<sup>\*</sup> Corresponding author. E-mail: [hatta.masayuki@ocha.ac.jp](mailto:hatta.masayuki@ocha.ac.jp)

<sup>†</sup> Present address: Research Center for Subtropical Fisheries, Seikai National Fisheries Research Institute, 148 Fukai-Ota, Ishigaki, Okinawa, Japan  
doi:10.2108/zs220043

cells (Hayward et al., 2001; Attenborough et al., 2019), the preferential vertical swimming along fairly straight paths may imply that the planulae might be equipped with some control mechanisms for swimming with respect to gravity. Whatever the mechanisms are, vertical swimming could play an important role in dispersal and settlement of planulae. In order to gain an insight into its roles, we demonstrate in this paper the active vertical swimming of coral larvae, which has not been fully investigated so far.

## MATERIALS AND METHODS

### Preparation of planulae

Fragments of colonies were collected for *Acropora tenuis* (Dana, 1846) at reefs around Sesoko Island (26°38'46"N, 127°51'54"E), Okinawa, Japan, under Okinawa prefectural government permission No. 26-9, 27-1. Five days prior to the full moon of the predicted spawning, the collected colony fragments were kept in an outdoor tank with a supply of running natural seawater until spawning at Sesoko Station of the University of the Ryukyus. When spawning occurred, buoyant bundles of eggs and sperm from the colony fragments were mixed together to allow fertilization, and reared in wide buckets by exchanging natural seawater every day at 27–29°C. Planulae 3.5 days after fertilization were packed in plastic bottles at density 3000 per liter and brought to the laboratory in Tokyo as luggage on an airplane. In the laboratory, planulae were maintained in wash-basins at density 1000–2000 per liter at around 26°C with daily exchanging of seawater. Seawater used in the laboratory was a 1:1 blend of artificial seawater (Coral Pro, RedSea) and natural seawater sterilized at 105°C for 3 minutes. Planulae 10 to 12 days after fertilization were used for recording of larval movement.

### Recording of larval movement

Vertical swimming of planulae was recorded in a vertical chamber with an inner dimension of 100H × 100W × 3D mm unless otherwise specified. The chamber was made of glass plates separated by a 3 mm-thick silicon rubber spacer. Twenty to 30 planulae were transferred into seawater in the chamber, and the quasi-planar swimming in the vertical space between two glass plates was recorded by a CMOS USB camera (UI-3240-CP-M-GL, IDS Imaging Development Systems GmbH, Obersulm, Germany) under transmission illumination by a CCFL backlight (light guiding panel equipped with a cold cathode fluorescent lamp) (a remodeling product of a flat light viewer, MedaLight LP-100, Minato Shokai Co., Yokohama, Japan) that was larger than the chamber and placed just behind the vertical chamber. Horizontal swimming was recorded using a 90-mm-φ petri dish with 5-mm-depth seawater.

In order to record the passive movement due to gravity, planulae after recording of vertical swimming were deciliated by immersion into hyperosmotic NaCl-seawater (3% [w/v] NaCl in seawater). One of the planulae was gently pipetted and transferred into NaCl-seawater. After the deciliation occurred within a few seconds, the planula, which became motionless, was then transferred to the normal seawater for washing. The deciliated planula, which was observed to have little deformation, was then transferred to a chamber with the inner dimension of 5 × 20 × 3 mm. In order to avoid adhesion of the planula, bovine serum albumin (BSA) was dissolved in sea water (0.1%, w/v) and glass surfaces were coated by agarose (0.05%, W/V). These procedures are widely adopted for observation of the motility of highly adhesive specimens, such as invertebrate sperm (Ohmuro et al., 2004) or isolated ciliated cells (Mogami et al., 1992). Planulae treated with NaCl-seawater regenerated their cilia several hours after the deciliation and restarted normal swimming.

While the chamber was placed horizontally prior to recording the sedimentation movement, a deciliated planula was placed on the glass wall of the chamber, usually beneath the top cover glass.

After turning the chamber upright, the vertical movement of a planula was recorded for several seconds by a horizontal video microscope equipped with a CCD camera (SONY XC-77, SONY, Tokyo, Japan) under darkfield illumination.

The sedimentation speed of fertilized eggs of *A. tenuis* was measured by a similar method, in which eggs were first accumulated at the top of the chamber and those floating were recorded in the chamber placed upside down.

All of the measurements were made at an ambient temperature of around 25°C.

The density and viscosity of seawater were  $1.021 \times 10^3 \text{ kg m}^{-3}$  and  $0.96 \times 10^{-3} \text{ Pa s}$ , respectively, and those of BSA-containing seawater were  $1.020 \times 10^3 \text{ kg m}^{-3}$  and  $0.97 \times 10^{-3} \text{ Pa s}$  (25°C), respectively. Kinematic viscosity of the medium was determined using an Ostwald viscosimeter with distilled-and-deionized-and-nanofiltrated water as the standard.

### Quantitative image analysis

Swimming trajectories were obtained by superimposing of planula's images that were recorded by video (30 fps) after adequately subtracting the background light density.

For details of swimming behavior, the recorded video images were analyzed frame by frame using the custom-made image analysis software, Bohboh (Bohbohsoft, Tokyo, Japan) (Shiba et al., 2005). Positions of planulae (coordinates of the center of the planular image) were calculated as "REAL" by least-squares pattern fitting. Swimming vectors were calculated from the changes in the position every  $n$  frames (usually  $n > 10$ ). Swimming speed,  $v$ , swimming direction,  $\theta$ , and orientation angle of planula's body fore-aft axis with respect to the gravity vector were calculated from the swimming vectors. 0 radians (0 degrees) means downward, and  $\pi$  radians (180 degrees) means upward. The final orientation angle was based on the last frame of the video just before planulae reached either the top of the chamber or the bottom. Turning rate of swimming direction at a given time was calculated as the slope of tangents of the plot of  $\theta$  against time (Fig. 7). The tangent was obtained by linear least-squares regression to the data including the corresponding point plus several neighboring points.

### Statistics

A bootstrap method was used for the estimation of the statistical significance of the difference between the upward and the downward propulsive speed. Bootstrap datasets were constructed based on 1000 resampling data sets. The bootstrap replications of the upward and the downward propulsive speed were calculated. The 99% confidence interval was estimated from the distribution of the differences between the upward and the downward propulsive speed obtained through the bootstrap. All of the procedures were carried out using R (R Core Development Team, 2017).

## RESULTS

### Basic swimming behavior of planulae

A planula has a body of roughly rotational symmetry around the fore-aft axis, although the aboral end is usually broader. Measurement of the immobilized planulae showed that the fore-aft axis was  $0.98 \pm 0.13 \text{ mm}$  (mean  $\pm$  S.D.,  $n = 44$ ) and the diameter of the broad aboral part was  $0.41 \pm 0.05 \text{ mm}$  ( $n = 45$ ). Planulae usually swim by ciliary beating with their broader aboral end in front (Fig. 1A). Backward swimming has never been observed.

Planulae swam in random directions in the shallow horizontal water layer with rolling (rotation around the fore-aft axis) and yawing/pitching (rotation around the axes perpendicular to the fore-aft axis). These rotational components caused planulae to swim along a helical trajectory (Fig. 1B). Planulae swam with variable speed (nearly zero to 2 mm

$s^{-1}$ ) which was observed to change abruptly.

### Vertical swimming of planulae

The planulae moved between the water surface and the bottom in a 200 mL cell-culture bottle (see supplementary Movie S1). Figure 2 shows the typical vertical swimming trajectories of the planulae observed in the same bottle. Many looked like straight lines or highly extended helices (with pitch angles mainly less than 0.3 radians), although a few

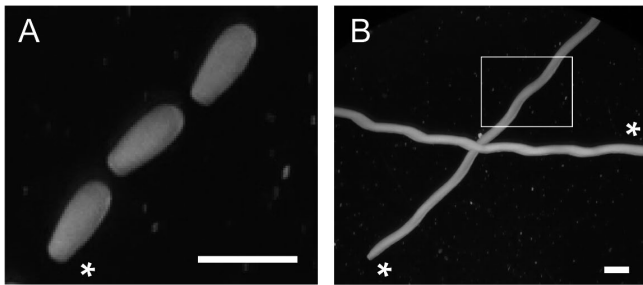


**Fig. 1.** The horizontal swimming behavior of planulae. **(A)** Magnified and superimposed still images at 1.5-second intervals of the swimming planula obtained from a video recording in the boxed area in **(B)**. **(B)** Trajectories of two planulae swimming in a Petri dish observed for 32.5 s. Asterisks show the beginning of each record. Scale bars, 1 mm.

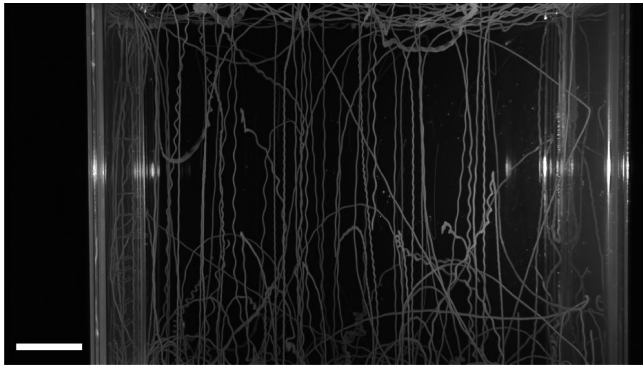


**Fig. 2.** Trajectories of the swimming of planulae observed in a cell culture bottle (80 mm wide  $\times$  30 mm deep  $\times$  90 mm high) for 10 minutes. Water surface is at the top of the figure. Scale bar, 10 mm.



**Fig. 3.** Trajectories of planulae swimming in a narrow upright chamber (200 mm wide  $\times$  3 mm deep  $\times$  200 mm high) for 10 minutes. Scale bar, 20 mm.

appeared to have larger pitch angles. Some sharp turns were occasionally observed between the nearly straight trajectories in opposite directions. This means that planulae swim preferentially upward or downward abruptly switched to swim in the opposite direction. Trajectories recorded in a quasi-vertical plane (Fig. 3) were similar as those in a 200 mL bottle (Fig. 2). During our observation, they didn't touch the glass walls when they swam vertically. Close-up observation using a horizontal microscope showed that planulae always swam with their aboral-end in front. When planulae were put into a larger setup (400H  $\times$  200W  $\times$  3D mm), they could continue to travel even 40 cm upward or downward along nearly straight swimming paths.

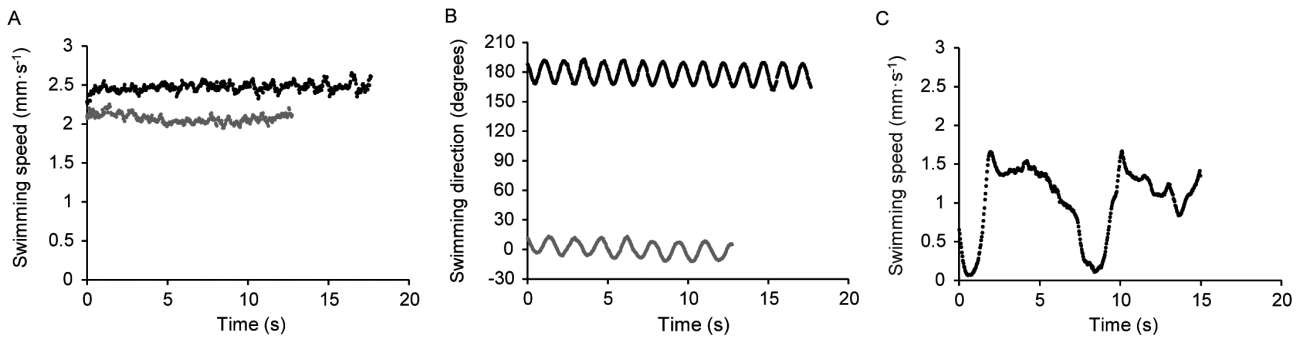
Figure 4 shows a typical example of time course plots of swimming speed and swimming direction for vertical as well as horizontal swimming. Planulae swam for a substantial period while maintaining their speed as well as the net vertical direction (Fig. 4A, B). The same results for speed and trajectory were obtained using a 200H  $\times$  200W  $\times$  5D mm chamber. This contrasts with the horizontal swimming, in which planulae frequently changed their speed (Fig. 4C). In a horizontal chamber, planulae tended to swim with the axis of the helical trajectory nearly parallel to the bottom or top surface of the horizontal water layer, even when they changed swimming speed. It is, therefore, not likely that a sudden decrease in the horizontal speed was caused by the change of swimming direction abruptly away from horizontal plane.

Figure 5A shows time course plot of sedimentation distance of a deciliated planula. The planula detached from the glass surface (0 to 10, Fig. 5B) rotated to orient its oral end upward (10 to 30), and steadily moved opposite to the gravity vector (30 to 60). These findings show that the planulae floated to the surface with a highly constant speed immediately after they attained the final oral-end-up posture. Twenty-two out of 25 deciliated planulae floated and three planulae sank. Twenty out of 25 deciliated planulae, such as the planula in Fig. 5B, converged their orientation into given angles as time passed. Figure 5C shows the distribution of deciliated planulae's final orientation ( $n = 25$ ) during passive movement. The median of the orientation was calculated at 174.4 degrees, which reflected the fact that the planula comes to adopt an oral-end-up posture during passive movement. These findings indicate that the planula is moving with a passive offset of buoyant force and rotational torque orienting itself toward the oral-end-up posture.

### Gravikinesis in the vertical movement

Swimming speed measured in upward and downward directions is summarized in Fig. 6A and B. Planulae swam with speed of  $2.44 \pm 0.39 \text{ mm s}^{-1}$  ( $n = 121$ ) and  $2.10 \pm 0.39 \text{ mm s}^{-1}$  ( $n = 122$ ) in the upward ( $180 \pm 5$  degrees) and downward ( $0 \pm 5$  degrees) directions, respectively. This indicates that planulae swim upward significantly faster than downward ( $t$ -test,  $P < 0.001$ ). When trajectories containing both upward and downward directions were selected in order to compare swimming speeds in single individuals, the upward swimming speed exceeded the downward speed in all of 10 cases and average speeds were  $2.74 \pm 0.39 \text{ mm s}^{-1}$  (upward) and  $2.10 \pm 0.34 \text{ mm s}^{-1}$  (downward).

Sedimentation experiments on the deciliated planulae



**Fig. 4.** Time course plots of swimming speed and swimming direction in a vertical chamber (**A**, **B**) and a horizontal chamber (**C**). Black and gray curves in (**A**) and (**B**) correspond to the swimming upward and downward of a single planula, respectively.

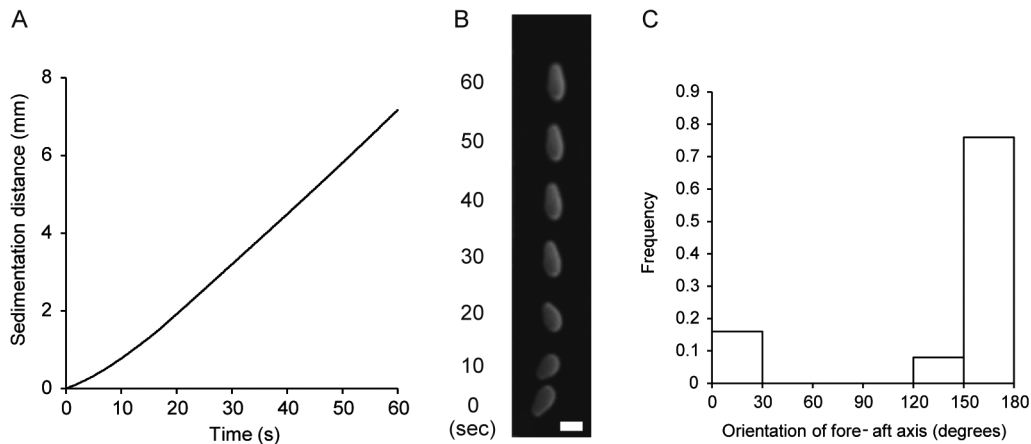


**Fig. 5.** Sedimentation of deciliated planulae. (**A**) Sedimentation distance as a function of time of a deciliated planula shown in (**B**). (**B**) Superimposed still images at 10-second intervals of a floating planula obtained from video recording. Scale bar, 0.5 mm. (**C**) Histogram of the deciliated planulae's final orientation ( $n = 25$  planulae) just before they reached either the top of the chamber or the bottom. Frequency is based on deciliated planulae. Orientation angle of the fore-aft body axis is measured with respect to the gravity vector (0 and 180 degrees corresponding to oral-down and oral-up orientation, respectively). Median of orientation is 174.4 degrees.

showed that they moved passively upward, although a few (three out of 25) were observed to move downward (Fig. 6C). This floatation (with speed of  $0.46 \pm 0.37 \text{ mm s}^{-1}$ ,  $n = 25$ ) would reflect the buoyant nature of the spawned egg from which the planulae developed.

Mechanical characteristics of swimming organisms can be characterized by a non-dimensional parameter, Reynolds number,  $Re = Ul/\nu$ , where  $U$  is speed,  $l$  is body length, and  $\nu$  is kinematic viscosity of the surrounding fluid. For planulae,  $l = 1.0 \times 10^{-3} \text{ m}$  and  $\nu = 0.95 \times 10^{-6} \text{ m}^2 \text{ s}^{-1}$  (kinematic viscosity of seawater of 3.5% salinity at 25°C). With  $U = 2.3 \times 10^{-3} \text{ m s}^{-1}$  (mean speed of the upward and downward swimming) and  $U = 4.6 \times 10^{-4} \text{ m s}^{-1}$  (mean passive speed of floating), planulae move actively at an  $Re$  of 2.4 and passively due to gravity at an  $Re$  of 0.48. These numbers are below the practical limit (about 5) for the situation in which the movement is amenable to being treated by the creeping motion equations (Happel and Brenner, 1983). In fact, deciliated planulae moved with constant speed during sedimentation (Fig. 5). These findings indicate that vertical movement of planulae is dominated mainly by viscous force with little contribution of inertial force.

For the viscosity-dominant motion under the influence of gravity, swimming velocity is determined by the vector sum

of the active propulsive velocity and passive sedimentation velocity (Machemer et al., 1991; Ooya et al., 1992; Takeda et al., 2006). Therefore, in the case of vertical swimming of planulae,

$$P_{dn} = v_{dn} + v_s \quad (1)$$

and

$$P_{up} = v_{up} - v_s \quad (2)$$

where  $v_{dn}$  and  $v_{up}$  are the magnitude of the velocity vector of the downward and upward swimming, respectively, and  $P_{dn}$  and  $P_{up}$  are the propulsive speed in the downward and upward directions, respectively, and  $v_s$  is the sedimentation speed, which is time-invariant and defined as positive when moving upward, as shown in Figs. 5A and 6C.

Gravikinesis is the regulation of propulsive thrust with respect to the gravity vector. It is, therefore, represented by the difference of propulsive speed ( $\Delta P = P_{dn} - P_{up}$ ); non-zero  $\Delta P$  gives strong evidence for gravikinesis. From equations 1 and 2,

$$\Delta P = (v_{dn} + v_s) - (v_{up} - v_s). \quad (3)$$

From the data shown above,  $\Delta P$  was calculated as  $0.58 \text{ mms}^{-1}$ .

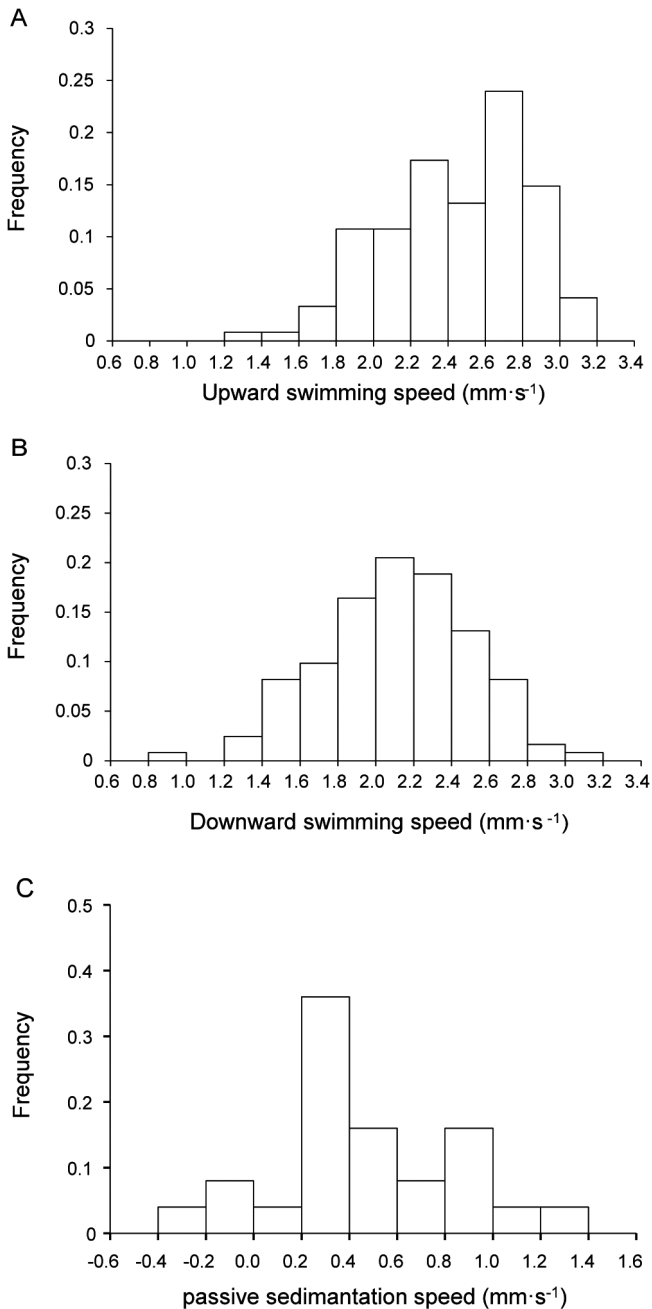


**Fig. 6.** Histogram of swimming speed and sedimentation speed. Speed data was obtained as the time average of values measured along each path. Frequency is based on the number of observed paths during upward ( $180 \pm 5$  degrees) swimming,  $n = 121$  (A) and during downward ( $0 \pm 5$  degrees) swimming,  $n = 122$  (B) and the number of deciliated planulae,  $n = 25$  (C). Downward movement is expressed in negative values and upward movement is expressed in positive values in (C).

$\Delta P$  was also estimated by a bootstrap method. A bootstrap enables the estimation of properties of a population by constructing a large number of sample datasets through random resampling and can be applied to almost any sample distributions for which it is difficult to assume a suitable formula (Efron and Tibshirani, 1994). The 99% confidence interval of  $\Delta P$  settled at between 0.4144 and 0.7736 (see

supplementary Figure S1); therefore, it is probable that  $\Delta P$  is significantly greater than zero, and thus  $P_{dn}$  is greater than  $P_{up}$ . This means that planulae have gravikinetic characteristics, in which planulae make greater effort of propulsion in the downward direction than in the upward direction.

It should be noted that  $v_{dn}$  and  $v_{up}$  were measured from the swimming vectors projected onto the vertical plane, which changed the direction along the helical swimming trajectory. This may lead to overestimation of the vertical component of the vectors. The overestimation, however, might not be large because pitch angles of the helix were relatively small ( $< 0.3$  radians) and the time-average of the measurement was used for representing  $v_{dn}$  and  $v_{up}$ .

### Orientation response

Sharp turns were observed in the vertical swimming but not in the horizontal swimming of planulae. There were very unique motile responses shown by gravitactic microorganisms. As shown in Fig. 3, planulae initially swimming downward or upward suddenly made sharp turns and swam in opposite directions. Planulae always swam with their aboral end in front during both turnings. The sharp turns were performed for tens of seconds between the preferential, relatively longer-lasting swimming in opposite directions.

Figure 7 shows the trajectories and the time course of swimming directions during the downward (Fig. 7A) and upward (Fig. 7C) turns. The insets are magnified images of the turning planulae at 0.5-second intervals. The orientation of a planula's body fore-aft axis almost agreed with its swimming direction. Maximum turning rates of the swimming direction were  $-0.29 \pm 0.11$  rad s<sup>-1</sup> ( $n = 9$ ) and  $0.28 \pm 0.11$  rad s<sup>-1</sup> ( $n = 14$ ), for downward and upward turns, respectively. As noted from the figure, trajectories of sharp turns did not have symmetrical geometry with respect to the gravity vector; the maximum turning rate was observed at the orientation angles of  $1.30 \pm 0.04$  rad ( $n = 9$ ) and  $1.36 \pm 0.08$  rad ( $n = 14$ ), for downward and upward turns, respectively.

## DISCUSSION

### Vertical swimming and gravikinesis of planulae

We reported in this paper unique vertical swimming of planulae of *A. tenuis*. Planulae were observed to swim preferentially upward or downward with almost constant speed and direction for long distances. In contrast to horizontal swimming, which shows frequent changes of speed and direction like a random walk when larvae are kept in petri dishes, vertical swimming is very stable in both the speed and direction. We focused on the swimming of planulae in a narrow space bounded by glass surfaces. This experimental design may introduce some physical constraints on the swimming behaviors. However, the fact that continuous vertical straight swimming was observed in the wide chamber and even in a bucket as well indicates that this unique behavior is not caused by the constraint derived from the narrow space of the recording chambers.

We also demonstrated that planula larvae have gravikinetic characteristics, in which planulae make greater effort of propulsion in the downward direction than in the upward direction. Narrow spacing between chamber walls, 3–5 mm space for 0.4 mm diameter planulae, may introduce another hydrodynamic "wall effect". Microorganisms may experience

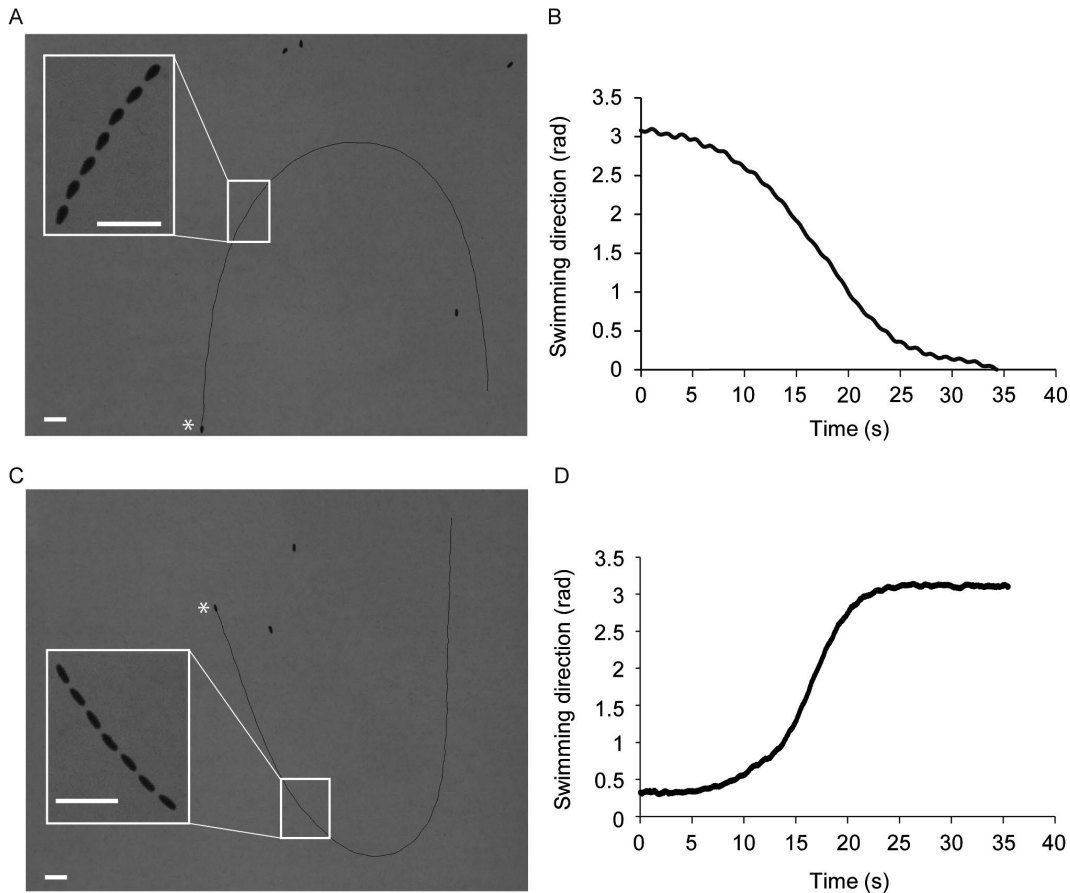


**Fig. 7.** Swimming trajectories and time course plots of sharp turns. **(A)** and **(C)** show swimming trajectories (solid black lines) during the downward and the upward turn, respectively, which were drawn by superimposing of the planula's images that were recorded by video (30 fps). The insets are magnified images at 0.5-second intervals of the turning planulae. **(B)** and **(D)** show the time course of swimming direction during the downward and the upward turn, respectively, which were obtained from the analyses of the trajectories in **(A)** and **(C)**. Asterisks show the start point of the trajectories. Scale bars, 3 mm.

larger viscous drag when swimming near the wall (Happel and Brenner, 1973; Vogel, 1994). As described in the Materials and Methods section, we measured passive sedimentation speed on the deciliated planulae that moved very near the glass surface. It is therefore possible that the sedimentation speed,  $v_s$ , used for calculating  $\Delta P$  (equations 1 to 3) is smaller than the speed estimated for the planulae swimming distantly from the chamber wall. This means that  $\Delta P$  would be correctly estimated to be a greater positive value, and our conclusion about the gravikinesis remains valid.

#### Estimation of planula body density

Because the gravitactic migration is performed under the strong bias of the passive sedimentation, it should be valuable to know the actual density of the gravitactic organisms.

In the sedimentation under low  $Re$  conditions, gravitational force is balanced by viscous force. Therefore, for a planula floating with a velocity  $v_s$  in the medium of viscosity  $\eta$ ,

$$Dv_s\eta = V\Delta\rho g, \quad (4)$$

where  $D$  is the coefficient of viscous resistance, and  $V$ ,  $\Delta\rho$ , and  $g$  are volume, density difference between the planula

( $\rho_p$ ) and seawater ( $\rho_{sw}$ ),  $\Delta\rho = \rho_{sw} - \rho_p$ , and gravity acceleration, respectively. If we consider the planula as a prolate spheroid sinking with its long axis parallel to the gravity vector,

$$V = \frac{4}{3}\pi r_a r_b^2, \quad (5)$$

and

$$D = \frac{8\pi e r_b}{\sqrt{1-e^2} \left\{ \frac{1+e^2}{2e^2} \ln\left(\frac{1+e}{1-e}\right) - \frac{1}{e} \right\}}, \quad (6)$$

where  $e$  is the eccentricity of the ellipsoid;

$$e = \sqrt{1 - (r_b/r_a)^2}, \quad (7)$$

where  $r_a$  and  $r_b$  are the major- and minor-axis radius (Happel and Brenner, 1983).

If we take  $r_a = 0.49$  mm,  $r_b = 0.21$  mm,  $\eta = 0.97 \times 10^{-3}$  Pa s (BSA-containing seawater), and  $v_s = 0.46$  mm s $^{-1}$ , we will obtain  $\Delta\rho = 2.53$  kg m $^{-3}$ . Since  $\rho_{sw} = 1.020 \times 10^3$  kg m $^{-3}$ ,  $\rho_p$  is calculated at  $1.0176 \times 10^3$  kg m $^{-3}$ .

The unfertilized egg of *A. tenuis* is almost a sphere and floats just after spawning. The radius of the egg and  $v_s$  were

measured as  $0.28 \pm 0.023$  mm and  $2.50 \pm 0.64$  mm s<sup>-1</sup> ( $n = 42$ ), respectively. These values are similar to those obtained from fertilized eggs of Caribbean coral, *Montastraea faveolata*, with a diameter of 300 to 350  $\mu$ m and  $v_s = 1.82$  mm s<sup>-1</sup>. (Szmant and Meadow, 2006). Assuming the egg as a sphere of radius  $R$ , and by putting  $V = (4/3)\pi R^3$  and  $D = 6\pi R$  (Stokes' law) in equation 4, we obtained  $\Delta\rho = 14.6$  kg m<sup>-3</sup> for *A. tenuis* and 34 kg m<sup>-3</sup> for *M. faveolata*. Harii et al. (2007) reported that *A. tenuis* egg and planula both contain a large amount of wax ester. The decrease in  $\Delta\rho$  above indicates that planulae are likely to consume during development the lipid which largely contributes to the positive buoyancy of planulae.

Detection of sedimentation equilibrium in medium with a density gradient is a direct measurement of the density, and was successful for specimens with density greater than the medium, such as echinoid (Pennington and Emler, 1986) and some sympatric Mediterranean octocoral larvae (Guizien et al., 2020). But it is not necessarily easy to apply this method to specimens with lower density. Although it is an indirect measurement, the estimation based on the hydrodynamic principle is a useful alternative method.

For the assessment of the sinking speed of the planula, we used deciliation. Deciliation will cause a reduction in the radii which determine the coefficient of the hydrodynamic drag,  $D$ . However, when the average length of cilia, about 15  $\mu$ m, is taken into consideration, changes in hydrodynamic radii,  $r_a$  and  $r_b$ , and the eccentricity,  $e$ , predict an increase in  $D$  for ciliated planula by about 6 percent and a reduction in the passive speed by about 5 percent. We confirmed that changes in  $v_s$  to this extent are so small that deciliation could give a safe estimate for gravikinesis of downward swimming planulae.

### Gravitactic turning

A unique characteristic of the vertical trajectory is the sharp turn frequently observed between the nearly straight swimming paths in opposite directions. As shown in Supplementary Movie S1, larvae once swimming preferentially upward or downward suddenly changed the course to the opposite direction. This means that the larvae swimming vertically switched abruptly their preference of the swimming direction with respect to gravity.

Migration of microorganisms with respect to gravity, which is referred to as gravitaxis, has long been studied, especially in unicellular organisms (Bean, 1984; Haeder et al., 2005). Accumulated evidence revealed that the gravitactic behavior of microorganisms should be characterized by two distinct responses to gravity, gravikinesis and orientational responses. Gravikinesis is the kinetic response modulating propulsive thrust depending on the swimming direction with respect to the gravity vector (Machemer, 1998). *Paramecium* is known to increase propulsive speed when swimming upward and reduces it when swimming downward (Machemer et al., 1991; Ooya et al., 1992; Takeda et al., 2006). Independently of the kinetic response, microorganisms show orientational responses in which they swim preferentially along the gravity vector. The orientation response appears on the basis of the generation of the orientation torque which changes the swimming direction with respect to gravity. The torque had been thought to be originated princi-

pally from the mechanical property of microorganisms (Bean, 1984; Mogami et al., 2001). Orientation response could also be supported by the physiological regulation of the propulsion with the aid of the specialized cellular mechanoreception (Fenchel and Finlay, 1984; Ooya et al., 1992; Mogami and Baba, 1998). Smooth turning trajectories shown in Fig. 7 suggest that gravitactic reorientation occurred depending on a static mechanical property of the larval body, e.g., body density and body shape, rather than a physiological ciliary response such as the ciliary reversals found in a ciliate *Loxodes* in response to gravity by using the Mueller vesicle as a sensor (Fenchel and Finlay, 1984), because there has been no evidence of a gravity sensor in coral larvae.

The Reynolds number for gravity-dependent orientation can be calculated as  $l^2\omega/\nu$ , where  $\omega$  is the angular velocity of the rotation, and again  $l$  is body length, and  $\nu$  is kinematic viscosity. We can estimate the average value of  $\omega$  as 0.3 rads<sup>-1</sup>. This gives  $Re$  less than unity (ca. 0.3) for the rotation. Under this low  $Re$  condition, gravity-dependent rotation can be caused by the torque generated on the basis of the fore-aft asymmetry in shape as well as that in density distribution. As schematically explained in Mogami et al. (2001), observation of the reorientation movement of a floating immobilized organism could show which is more dominant: the torques based on the shape-asymmetry or that based on the density-asymmetry. Figure 5 shows a deciliated-floating planula larva rotated broad aboral end down, as in the case of sea urchin pluteus that rotated large oral side down when floating in hyperdensity Percoll-containing sea water (Mogami et al., 2001). It is, therefore, highly likely that the gravitactic orientation is predominantly biased by the fore-aft asymmetry of density distribution rather than the asymmetry of the body shape.

Because the planula larva contains a large amount of low density substances (mainly wax ester), uneven distribution of the substance(s) may lead to separating the center of gravity from that of buoyancy. The separation could be estimated by assuming the problem as the rotation of the ellipsoidal body of a larva around its minor axis. Because we assume the planula as a rotating ellipsoid, the centers of gravity and buoyancy are located on the long axis, and the center of the drag for translational movement is located on the center buoyancy; the simplest case of minor contribution of the shape-asymmetry.

Following the theory of mechanical orientation under low Reynolds number condition, rotation speed,  $d\theta/dt$ , is proportional to the torque around the center of the body,  $T$  (Roberts, 1972; Mogami et al., 2001). They are formulized as

$$\frac{d\theta}{dt} = \beta \sin \theta \quad (8)$$

and

$$T = LV\rho_l g \sin \theta \quad (9)$$

where  $\theta$  is orientation angle, i.e., the angle of the long axis with respect to the gravity,  $\beta$  is the maximum rotation rate, and  $L$  is the lever length of the moment of couple forces, gravity and buoyancy. Therefore,

$$R\beta \sin \theta = LV\rho_l g \sin \theta \quad (10)$$



where  $R$  is a proportional factor defined as,

$$R = 8\pi r_a r_b^2 \eta C_M \quad (11)$$

where  $C_M$  is a function of the eccentricity of the ellipsoid,  $e$  (Chwang and Wu, 1974),

$$C_M = \frac{4e^3(2-e^2)}{3(1-e^2) \left\{ -2e + (1+e^2) \ln \left( \frac{1+e}{1-e} \right) \right\}} \quad (12)$$

Based on the simple assumption that the fore-aft body axis is just on the swimming vector, we can estimate the rotation speed from the turning rate of swimming direction. When we take  $\beta = 0.28$  and  $0.29 \text{ rad s}^{-1}$  for downward and upward turns, respectively, and  $\rho_l = 1.018 \times 10^3 \text{ kg m}^{-3}$ ,  $\eta = 0.97 \times 10^{-3} \text{ Pa s}$  and  $e = 0.93$ , we obtain  $L = -0.29 \times 10^{-6}$  and  $0.29 \times 10^{-6} \text{ m}$  for downward and upward turns, respectively. This means that the center of gravity is located about  $0.3 \mu\text{m}$  anterior and  $0.3 \mu\text{m}$  posterior to the center of buoyancy for downward- and upward-turning larvae, respectively. These are much smaller than the total length of the larva, and may suggest that the sign of gravitaxis can be changeable in response to the shift of the center of the reaction forces as a result of a minor change in either the internal or external geometry of the larva. Plasticity of the geometry of the larval body may be reflected by the two peaks found in the histogram of the final orientation of the deciliated larvae (Fig. 5C).

### Migration-settlement scenario revised

The speeds of tidal currents and orbital wave motions are much greater than coral larval swimming speeds (Hata et al., 2017), and one may think that larval swimming does not contribute to dispersal and settlement. However, seawater never shows evermoving flows and currents. Seawater movements fluctuate according to climate conditions and other factors; for example, seawater stops in reef flats for awhile at the turn of the tide on calm days. A more important aspect is the patchy structures of seawater, water masses. Water masses are formed at various scales, from fine scale (tens of meters) to mesoscale (hundreds of kilometers), and sometimes enclose planktons of particular compositions according to the nutrients (e.g., De Verneil et al., 2019). Water masses are rather stable and need strong forces to be mixed, and thus act as cages for plankton. Coral larvae may also be caught in water masses and conveyed by large-scale water flows. Larval vertical swimming will be efficient in each water mass, in which water movements are very slow as still water. Inside water masses, vertical swimming will allow coral larvae to reach the sea bed quickly or to depart from unfavored substrates to the sea surface for the next attempt at dispersal and settlement. Thus, the unique bimodal gravitactic behavior of planula larvae is highly worth investigating from the ecological as well as biomechanical point of view.

During dispersal, planulae consume lipid resources, which mainly consist of wax ester (Harui et al., 2007). It has been thought simply that consumption of this wax ester causes buoyancy reduction and makes the planulae sink gradually to the bottom. In this view, planulae have only a single chance to seek their settlement positions. The gravitactic and gravikinetic characteristics shown in this study suggest that planulae shuttle between the sea surface and the bottom and can attempt settlement multiple times after drifting around the surface for a certain period following failure to encounter appropriate environments at the sea bed. This scenario enables higher efficiency of dispersal and settlement than previously supposed.

actic and gravikinetic characteristics shown in this study suggest that planulae shuttle between the sea surface and the bottom and can attempt settlement multiple times after drifting around the surface for a certain period following failure to encounter appropriate environments at the sea bed. This scenario enables higher efficiency of dispersal and settlement than previously supposed.

### CONCLUSION

We reported in this study downward and upward straight swimming of planulae of acroporids, with direction switching. These shuttle movements between top and bottom through the water column were observed especially when rearing planulae in undisturbed water. We have characterized gravikinesis and gravitactic reorientation of the swimming, although the detailed mechanism of the gravity-dependent regulation of swimming speed and generation of the gravitactic orientation torque is still unclear. Further investigation of the gravitaxis of the planulae will help us understand the strategy to extend the habitat of the reef-building corals, which play significant roles in marine ecosystems.

### ACKNOWLEDGMENTS

Authors express special thanks to Professor Kei Yura and Ms. Minori Ooshima, Ochanomizu University, for their technical help for bootstrapping analysis, to Ms. Katherine Georgopoulos at Executive Language Training in Chicago for English editing advice, and to the technical staff at Sesoko Station and Dr. Yusuke Sakai for help for collecting corals.

### COMPETING INTERESTS

The authors declare no competing interests.

### AUTHOR CONTRIBUTIONS

ATS, JH, SS, and KM collected data. ATS, SAB, YM, and MH analyzed data, made interpretations, and wrote the manuscript.

### SUPPLEMENTARY MATERIALS

Supplementary materials for this article are available online. (URL: <https://doi.org/10.2108/zs220043>)

**Supplementary Movie S1.** Vertical swimming behavior of planulae in a large upright container (80 mm wide  $\times$  30 mm deep  $\times$  90 mm high) for 10 minutes.

**Supplementary Figure S1.** The distribution of  $\Delta P$  obtained by the bootstrap method based on 1000 resampling data sets.

### REFERENCES

- Arai T, Kato M, Heyward A, Ikeda Y, Iizuka T, Maruyama T (1993) Lipid composition of positively buoyant eggs of reef building corals. *Coral Reefs* 12: 71–75
- Attenborough RMF, Hayward DC, Wiedemann U, Forêt S, Miller DJ, Ball EE (2019) Expression of the neuropeptides RFamide and LWamide during development of the coral *Acropora millepora* in relation to settlement and metamorphosis. *Dev Biol* 446: 56–67
- Bean B (1984) *Membranes and Sensory Transduction*. Plenum Press, London
- Chwang AT, Wu TY (1974) Hydromechanics of low-Reynolds-number flow. Part 1. Rotation of axisymmetric prolate bodies. *J Fluid Mechanics* 63: 607–622
- De Verneil A, Franks PJS, Ohman MD (2019) Frontogenesis and the creation of fine-scale vertical phytoplankton structure. *J Geophys Res Oceans* 124: 1509–1523
- Efron B, Tibshirani RJ (1994) *An Introduction to the Bootstrap*.

- Chapman and Hall/CRC, New York
- Fenchel T, Finlay B (1984) Geotaxis in the ciliated protozoan *Loxodes*. *J Exp Biol* 110: 17–33
- Guizien K, Viladrich N, Martinez-Quintana A, Bramanti L (2020) Survive or swim: different relationships between migration potential and larval size in three sympatric Mediterranean octocorals. *Sci Rep* 10: 18096
- Haeder D, Hemmersbach R, Lebert M (2005) Gravity and the Behavior of Unicellular Organisms. Cambridge University Press, New York
- Happel J, Brenner H (1986) Low Reynolds Number Hydrodynamics. 2nd ed, Martinus Nijhoff Publishers, Dordrecht
- Harii S, Nadaoka K, Yamamoto M, Iwao K (2007) Temporal changes in settlement, lipid content and lipid composition of larvae of the spawning hermatypic coral *Acropora tenuis*. *Mar Ecol Prog Ser* 346: 89–96
- Hata T, Madin JS, Cumbo VR, Denny M, Figueiredo J, Harii S, et al. (2017) Coral larvae are poor swimmers and require fine-scale reef structure to settle. *Sci Rep* 7: 2249
- Hayward DC, Catmull J, Reece-Hoyes JS, Berghammer H, Dodd H, Hann S, Miller DJ, Ball EE (2001) Gene structure and larval expression of *cnx-2Am* from the coral *Acropora millepora*. *Dev Genes Evol* 211: 10–19
- Machemer H (1998) Mechanisms of graviperception and response in unicellular systems. *Adv Space Res* 21: 1243–1251
- Machemer H, Machemer-Roehnsch S, Braeucker R, Takahashi K (1991) Gravikinesis in *Paramecium*: theory and isolation of a physiological response to the natural gravity vector. *J Comp Physiol A* 168: 1–12
- Martinez-Quintana A, Bramanti L, Viladrich N, Rossi S, Guizien K (2015) Quantification of larval traits driving connectivity: the case of *Corallium rubrum* (L. 1758). *Mar Biol* 162: 309–318
- Mogami Y, Baba SA (1998) Super-helix model: a physiological model for gravitaxis of *Paramecium*. *Adv Space Res* 21: 1291–1300
- Mogami Y, Sekiguchi S, Baba SA (1992) Beating of cilia of sea urchin embryos: A critical comparison of the normal and reversed beating of cilia of isolated cells. *J Exp Biol* 175: 251–266
- Mogami Y, Ishii J, Baba SA (2001) Theoretical and experimental dissection of gravity-dependent mechanical orientation in gravitactic microorganisms. *Biol Bull* 201: 26–33
- Morse ANC, Iwao K, Baba M, Shimoike K, Hayashibara T, Omori M (1996) An ancient chemosensory mechanism brings new life to coral reefs. *Biol Bull* 191: 149–154
- Nakajima Y, Nishikawa A, Iguchi A, Sakai K (2012) Regional genetic differentiation among northern high-latitude island populations of a broadcast-spawning coral. *Coral Reefs* 31: 1125–1133
- Ohmuro J, Mogami Y, Baba SA (2004) Progression of flagellar stages during artificially delayed motility initiation in sea urchin sperm. *Zool Sci* 21: 1099–1108
- Ooya M, Mogami Y, Izumi-Kurotani A, Baba SA (1992) Gravity-induced changes in propulsion of *Paramecium caudatum*: a possible role of gravireception in protozoan behavior. *J Exp Biol* 163: 153–167
- Pennington JT, Emler RB (1986) Ontogenetic and die1 vertical migration of a planktonic echinoid larva, *Dendroaster excentricus* (Eschscholtz): occurrence, causes, and probable consequences. *J Exp Mar Biol* 104: 69–95
- R Core Development Team (2017) R: a language and environment for statistical computing and graphics. R Foundation for Statistical Computing, Vienna, Austria URL: <https://www.R-project.org/> Accessed 11 March 2022
- Roberts AM (1970) Geotaxis in motile microorganisms. *J Exp Biol* 53: 687–699
- Shiba K, Ohmuro J, Mogami Y, Nishigaki T, Wood CD, Darszon A, et al. (2005) Sperm-activating peptide induces asymmetric flagellar bending in sea urchin sperm. *Zool Sci* 22: 293–299
- Storlazzi CD, van Ormondt M, Chen Y, Elias EPL (2017) Modeling fine-scale coral larval dispersal and interisland connectivity to help designate mutually-supporting coral reef marine protected areas: Insights from Maui Nui, Hawaii. *Front Mar Sci* 4: 381
- Takeda A, Mogami Y, Baba SA (2006) Gravikinesis in *Paramecium*: Approach from the analysis on the swimming behavior of single cells. *Biol Sci Space* 20: 44–47
- Vogel S (1994) Life in Moving Fluids: The Physical Biology of Flow. 2nd ed, Princeton University Press, Princeton

(Received April 28, 2022 / Accepted August 23, 2022 /

Published online October 12, 2022)